

# Supplemental Information : Understanding the nanoscale structure of hexagonal phase lyotropic liquid crystal membranes

Benjamin J. Coscia      Douglas L. Gin      Richard D. Noble      Joe Yelk  
Matthew Glaser      Xunda Feng      Michael R. Shirts

January 9, 2018

## Further details regarding monomer parameterization

Monomers were parameterized according to the following procedure:

1. *Create monomer structure file with connectivity* : We drew atomistic structures using MarvinSketch 17.13 with all hydrogen atoms drawn out explicitly. We optimized the 3D geometry of the structure using the 'Clean in 3D' function of MarvinSketch 17.13 [1]. We saved the structure as a .mol file, then converted it to .pdb format using Open Babel 2.4.1 [2, 3].
2. *Assign GAFF atomtypes using antechamber* : Using the .pdb structure file as input, we ran `antechamber` [4] using the AM1-BCC charge model. The net charge on the monomer is input as -1 since the sodium ion will be kept as a separate residue. The output of `antechamber` is used to create Amber topology files with LEaP [5]. A detailed tutorial can be accessed elsewhere [6].
3. *Create gromacs topologies from Amber output* : LEaP outputs a .inpcrd and a .prmtop file which are Amber topology files. Using acpype.py [7], we convert the LEaP output into GROMACS .gro and .top files.
4. *Perform a simulated annealing procedure on the monomer* : We created a cubic box around the monomer using the GROMACS command `gmx editconf`. The monomer was centered in the monomer in the box with edges of the box at least 3 nm from the monomer on all sides. We ran an energy minimization on the system with the steepest descent algorithm. Next we performed an NVT simulated annealing procedure. We linearly decreased the temperature of the system from 1000K to 50K over the course of 10 ns. We randomly chose a monomer configuration from the last 10 % of the trajectory.
5. *Reassign charges with molcharge* : With the monomer configuration taken from the annealed trajectory, we reassigned charges using `molcharge` using the am1bccsym method in order to ensure charges are symmetric. This condition is not guaranteed with `antechamber`. The charges in the gromacs topology file (.top) were replaced with the new charges calculated by `molcharge`.
6. *Anneal again to get final structure* : The same simulated annealing process was repeated using the monomer topology with `molcharge` charges. A random monomer configuration was pulled from the last 10 % of the trajectory and was used to build all assemblies reported (Figure 2).

### Calculation of pore-to-pore spacing statistics

This is an outline of this section and will be reworded for clarity

- We are interested in 5 pore-to-pore distances which should all be equal in a perfect hexagonal array, however only 4 distances are independent clear below.
- Each pore spacing has its own trajectory of spacing vs. time. Using data collected after the system is equilibrated, we calculate how long it takes for the data in each of the 5 trajectories to become uncorrelated using `pymbar.timeseries.integratedAutocorrelationTime()`

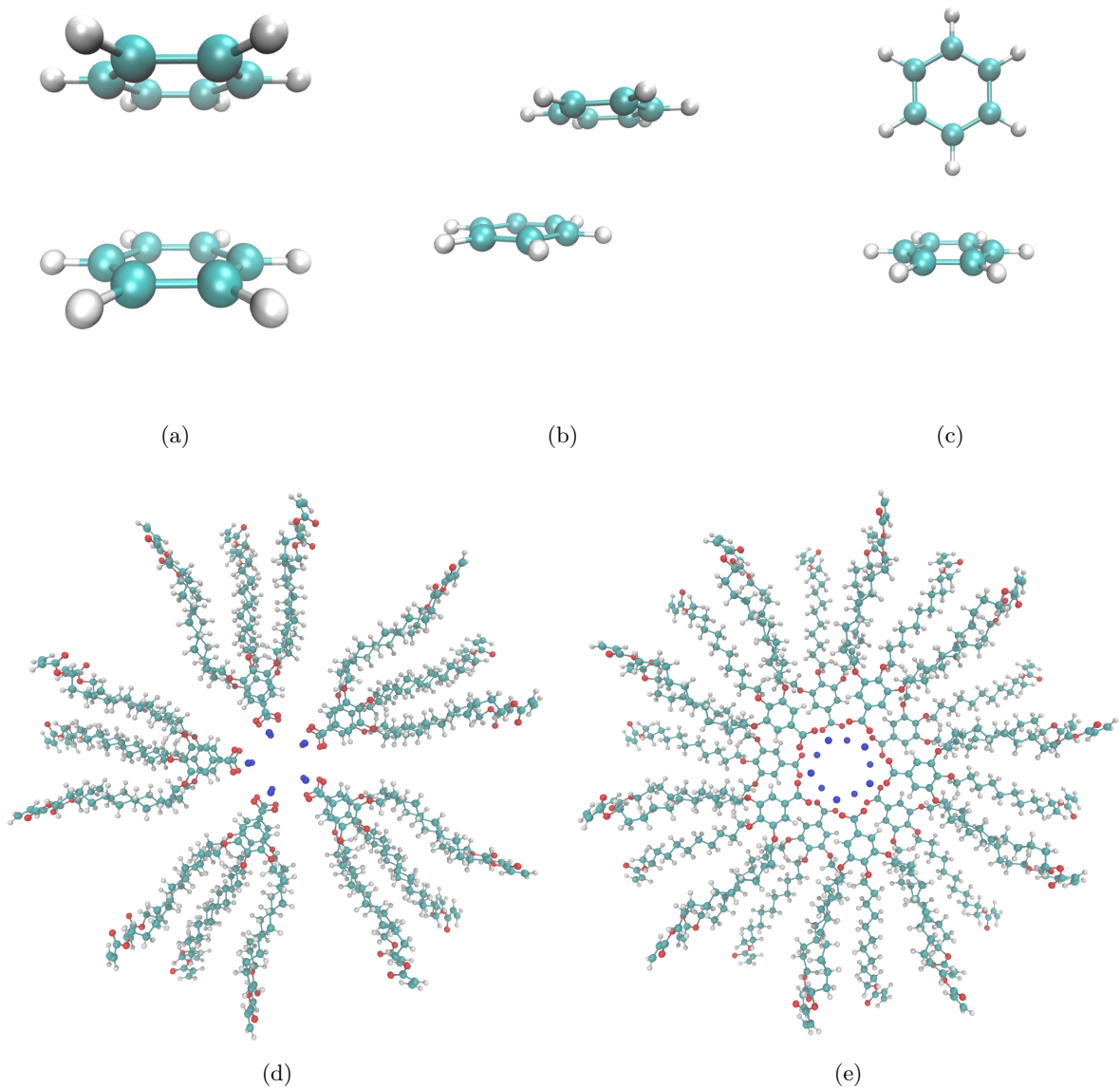


Figure 1: (a) Sandwiched benzene dimers stack 3.8 Å apart. (b) Parallel-Displaced benzene dimers stack 3.4 Å vertically and 1.6 Å horizontally apart. (c) T-shaped benzene dimers stack 5.0 Å apart. (d) Two monomer layers stacked in the sandwiched configuration (e) Two monomer layers stacked in the parallel-displaced configuration

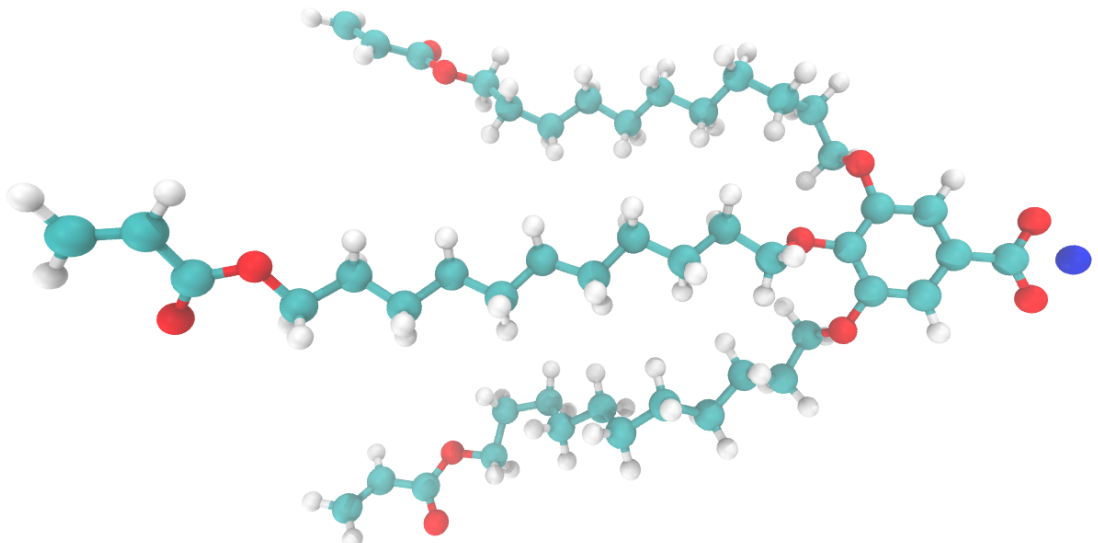


Figure 2: Atomistic representation of the monomer Na-GA3C11. White atoms represent hydrogen, cyan atoms represent carbon, red atoms represent oxygen and the blue atom is sodium.

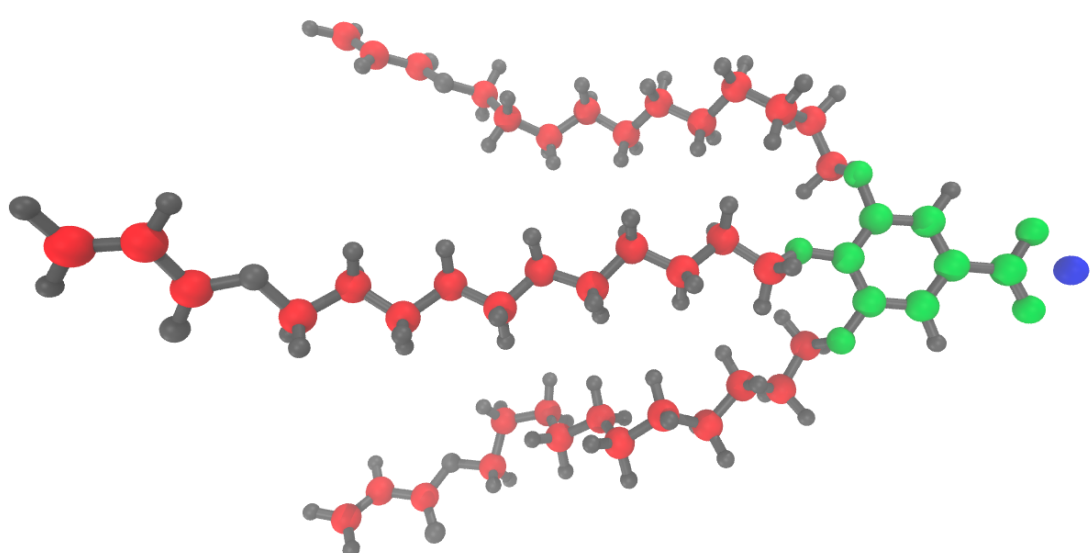


Figure 3: The groups used for  $g(z)$  calculations. Red atoms are in the tails group. Green atoms are in the head group region. The blue atom is sodium.

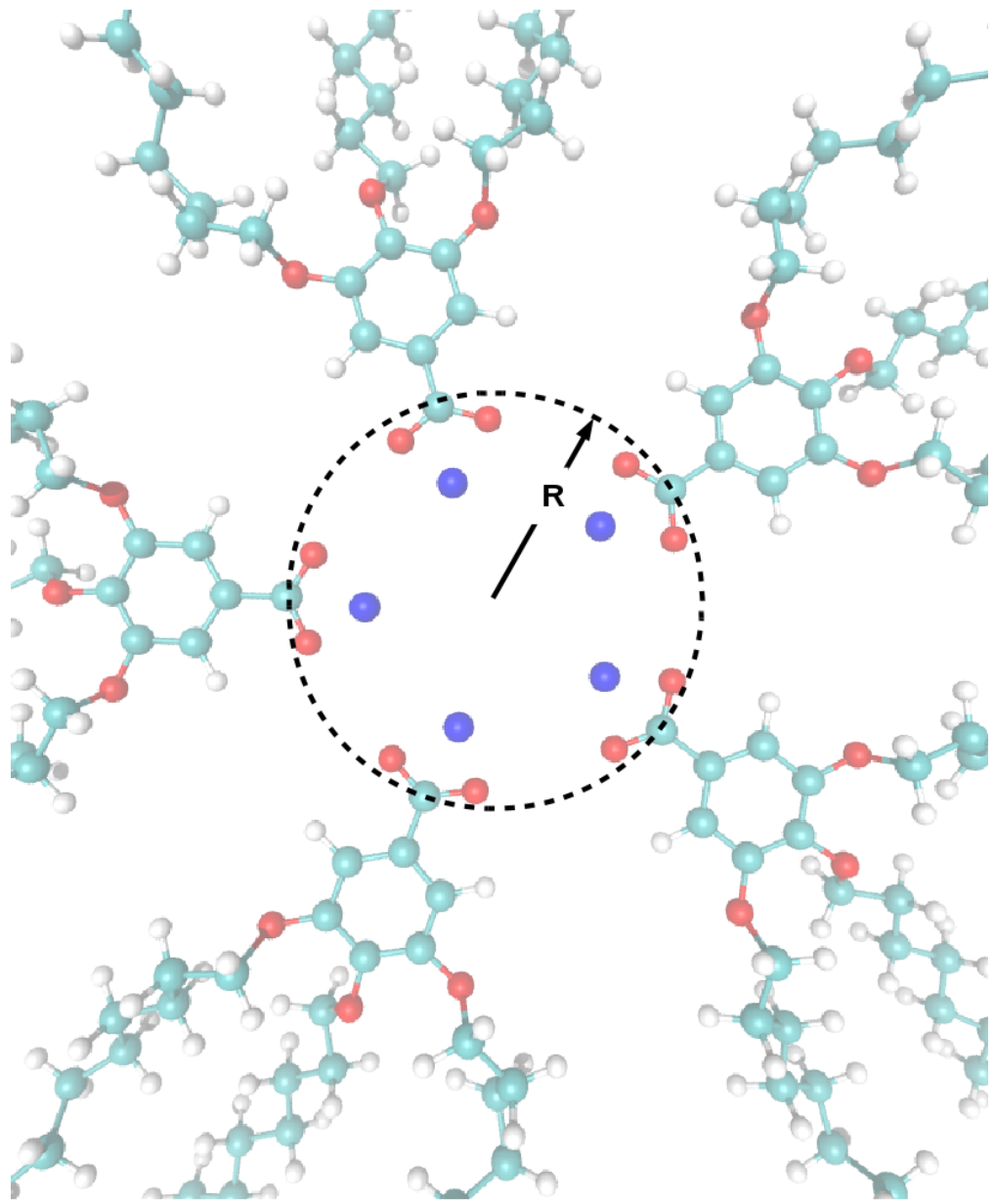


Figure 4: When creating an initial configuration, the pore radius is defined based on the distance of the carbonyl carbon from the pore's central axis

- We break the full trajectories down into sub-trajectories based on the maximum autocorrelation time of those found in the previous step.
- For each bootstrap trial, we recreate an equilibrium trajectory by randomly sampling pore spacings from the sub-trajectories
- We get an average value for each pore spacing by finding the mean of the bootstrapped data
- We calculate the overall average as the mean of all bootstrapped pore spacings
- The uncertainty for each pore spacing is calculated as  $\frac{\langle x \rangle - x}{4}$  where  $\langle x \rangle$  is the average spacing from the bootstrap trial and  $x$  is the average value of one of the pore spacings.
- We report the mean of these uncertainties

## Initial Configuration Dependence

Any major dependence on initial configuration is addressed in the main text. There we showed that systems are stable when made with 4, 5, 6, 7, and 8 monomers per layer. We also showed that systems are stable when monomer head groups are oriented in the parallel displaced and sandwiched configurations (See Figure 1). Our model best supports a system built with 5 monomers per layer in the sandwiched configuration.

There are three other parameters whose choice may influence the equilibrium structure: initial pore spacing, initial pore radius and initial distance between layers. Here we show the results of a sensitivity analysis performed on the three parameters. To reduce the size of the sensitivity analysis, we only tested systems built with 5 monomers per layer with layers stacked in the parallel displaced configuration. All systems were equilibrated according to the dry equilibration procedure.

### 1. Initial pore spacing

We tested five different initial pore spacings, defined as the distance between the central axis of each pore with all others. To reduce the number of variables, we held the pore radius constant, at 5 Å and the distance between layers at 3.7 Å since those were the values used in our optimal system in the main text. If the initial pore spacing is chosen to be too small, pore columns abruptly repel each other as soon as they are able to overcome the restraining potential present as part of the dry equilibration procedure. We avoided using systems that exhibit this behavior since the behavior increases the chances of a system to become kinetically trapped in an undesired metastable free energy basin.

- (a) 39 Å : A pore spacing of 39 Å is used in order to have a test system started with a spacing below the experimental value. As soon as the restraining potential switches to 56 KJ mol<sup>-1</sup> nm<sup>-2</sup>, the columns are able to separate resulting in a large jump in pore spacing (Figure 5a).
- (b) 41 Å : A pore spacing of 41 Å is chosen since it closely matches the experimental pore spacing. Again, we observe abrupt repulsion of columns once the restraining potential is switched to 56 KJ mol<sup>-1</sup> nm<sup>-2</sup> (Figure 5b).
- (c) 45 Å : A pore spacing of 45 Å is about 10 % larger than the experimental value. We observe relatively stable pore spacing during the restrained portion of the dry equilibration procedure (Figure 5c). We chose to use this value for all our simulations in the main text.
- (d) 50 Å : We tested a pore spacing of 50 Å, about 20 % larger than the experimental value. Once the restraining potential reaches 56 KJ mol<sup>-1</sup> nm<sup>-2</sup>, the pore spacing begins to decrease linearly (Figure 5d).
- (e) 55 Å : We tested a pore spacing of 55 Å which is at a distance where monomers in each pore no longer intersect adjacent pores. Once the restraining potential reaches 56 KJ mol<sup>-1</sup> nm<sup>-2</sup>, the pore spacing changes erratically until it begins to settle once the force constants are below 3 KJ mol<sup>-1</sup> nm<sup>-2</sup> (Figure 5e). We recommend avoiding a system such as this where vacuum gaps are introduced unnecessarily. The system equilibrates to a pore spacing of  $4.27 \pm 0.06$  nm.

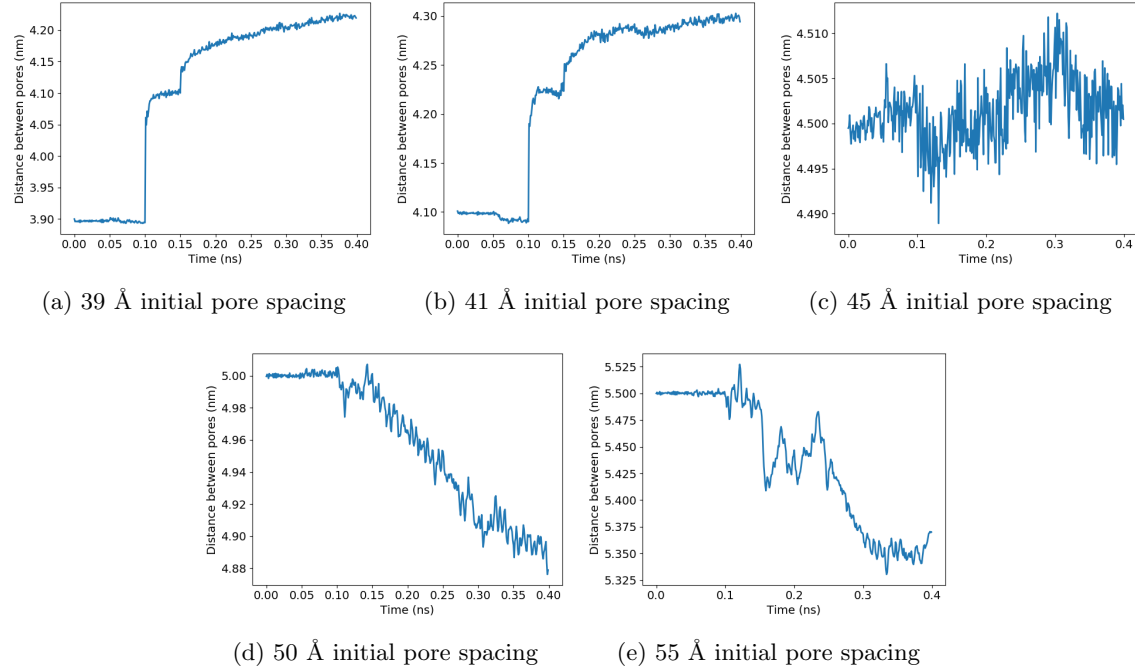


Figure 5: The pore spacing during the restrained portion of the dry equilibration procedure is shown. Every 50 ps (0.05 ns) position restraints are reduced according to the sequence: 1000000, 3162, 56, 8, 3, 2, 1, 0 KJ mol<sup>-1</sup> nm<sup>-2</sup>. When the initial pore spacing is chosen below the experimental value (a) or at the experimental value (b), there is an abrupt change in pore spacing when the position restraints are reduced to 56 KJ mol<sup>-1</sup> nm<sup>-2</sup>. When pores are started 45 Å apart (c) the pore spacing remains relatively stable. When pores are spaced 50 Å apart (d), the pore spacing decreases nearly linearly once the restraints are reduced to 56 KJ mol<sup>-1</sup> nm<sup>-2</sup>. When pores are spaced 55 Å apart (e), so that monomers do not intersect with adjacent pores, and position restraints are reduced to 56 KJ mol<sup>-1</sup> nm<sup>-2</sup>, pore spacing changes erratically before stabilizing when force constants are reduced to 3 KJ mol<sup>-1</sup> nm<sup>-2</sup>.

## 2. Initial pore radius

We tested 3 different pore radii, defined as shown in Figure 4. For each system, we held the initial pore spacing constant at 45 Å and the distance between layers constant at 3.7 Å. Equilibrated values of pore radii are presented in Table 1. The pore radius in each frame is calculated as the average distance of all carbonyl carbons (See Figure 4) from their associated pore center. Statistics for the pore radii reported were generated from the timeseries representing the average pore radius at each frame. Equilibration was detected using `pymbar.timeseries.detectEquilibration`. The average and standard deviation of pore radii were calculated using only data points collected after equilibration was detected.

- (a) 2.5 Å : The smallest pore radius that we can achieve before energy minimization becomes problematic is 2.5 Å.
- (b) 5 Å :
- (c) 8 Å : The largest pore radius that can achieve before energy minimization becomes problematic is 8 Å.

Initial Pore Radius	Equilibrated Pore Radius
2.5 Å	$0.394 \pm 0.002$ Å
5 Å	$0.423 \pm 0.002$ Å
8 Å	$0.721 \pm 0.002$ Å

Table 1: Caption of the future!

## 3. Initial distance between layers

We tested 3 different initial layer spacings, defined as the distance between the planes of aromatic rings in each layer. Systems built with layers stacked 3.7 Å and 5 Å apart are discussed extensively in the main text. We will focus the discussion here on systems built with layers stacked 10 Å apart.

Figure 6 shows the structure of an assembly built with an initial layer spacing of 10 Å immediately after the restrained portion of the equilibration procedure. Since position restraints, the simulations are run in the NVT ensemble. When layer spacing is large, such as this situation, there is a significant amount of vacuum space which the monomer attempts to fill. Even if turning pressure control on allows the system to recover the geometry of the hexagonal phase, we would likely need much longer equilibration times, and it will almost certainly remain trapped in metastable configurations that bear no resemblance to experimental profiles.

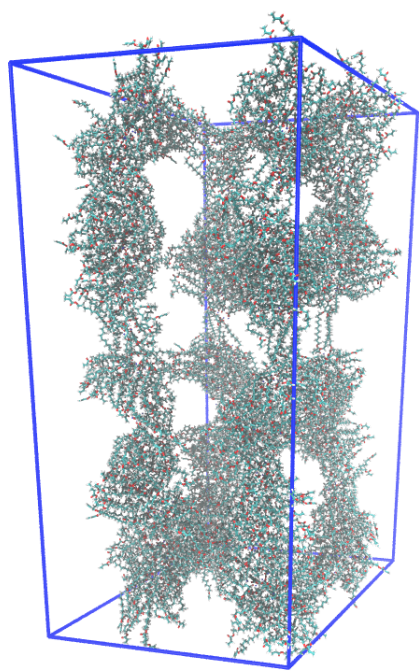


Figure 6

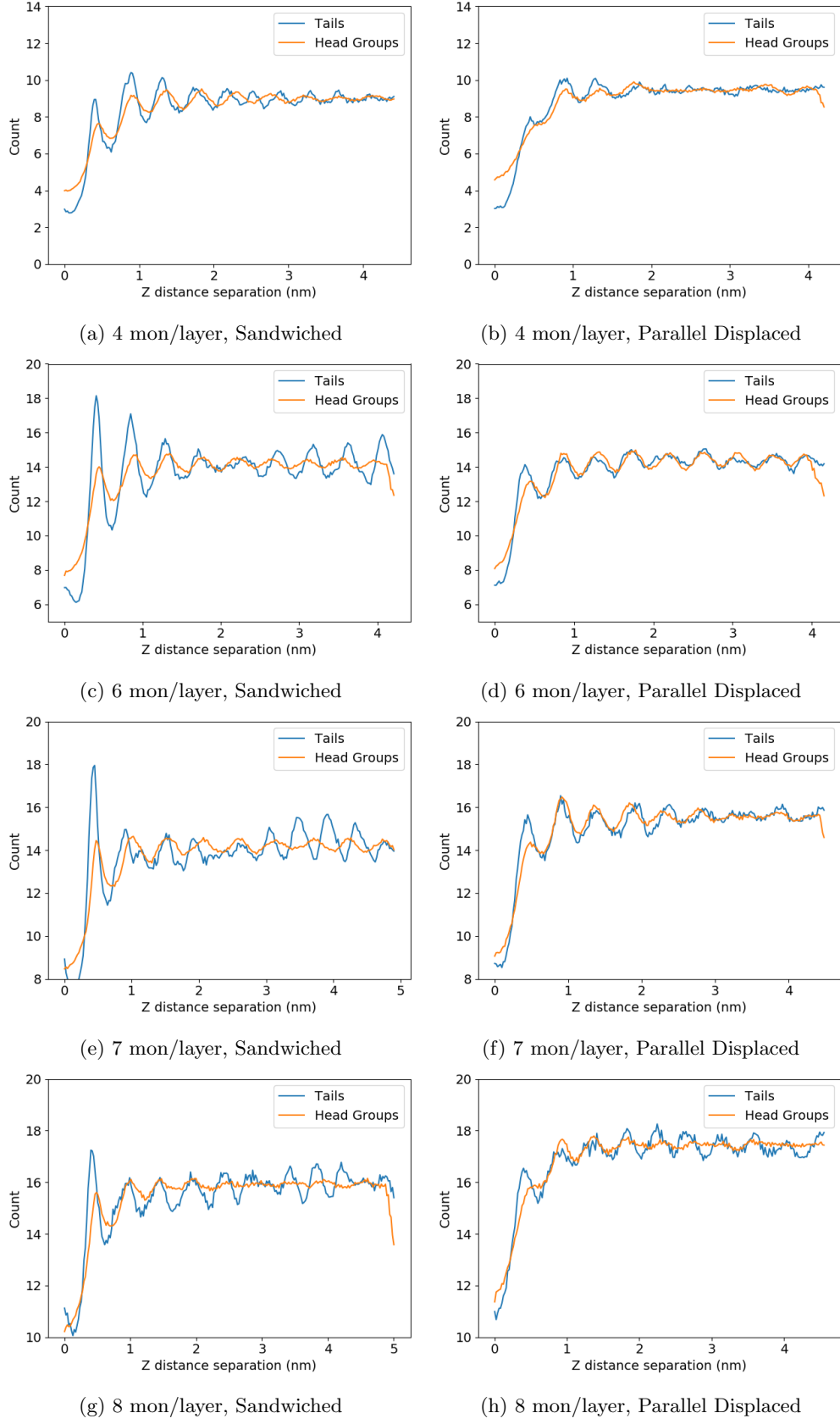


Figure 7:  $g(z)$  for all other configurations built with layers stacked 3.7 Å apart

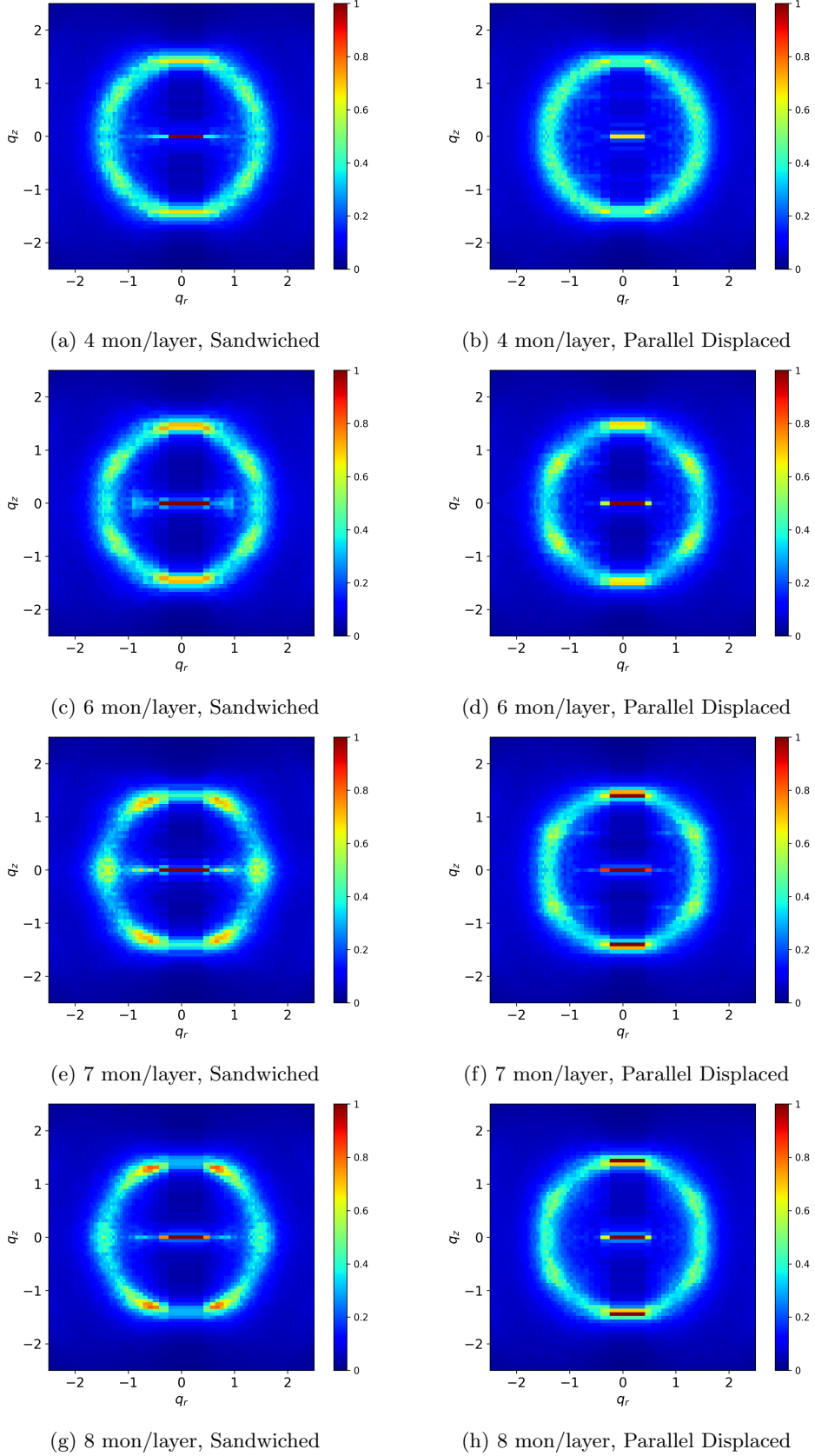


Figure 8: Simulated XRD patterns for all other configurations built with layers stacked 3.7 Å apart

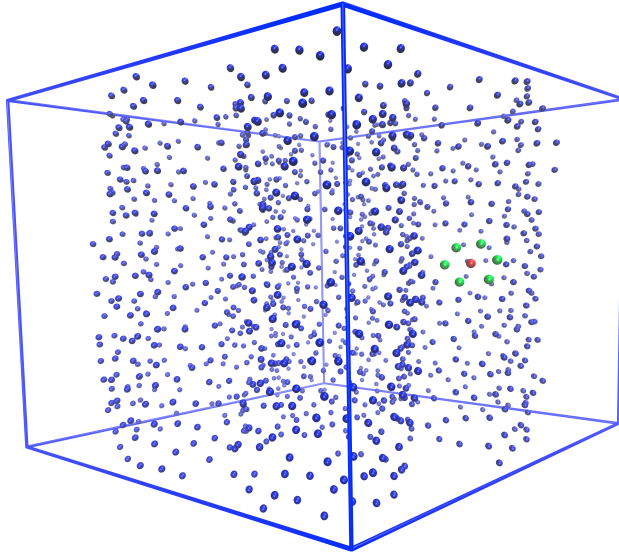


Figure 9: Monomer tails pack together hexagonally. The centroid of each tail is visualized as a blue sphere. The centroids are calculated based on the red atoms in Figure 3. The red sphere highlights an example of an alkane tail centroid with its nearest neighbors (green spheres) surrounding it in a hexagonal pattern.

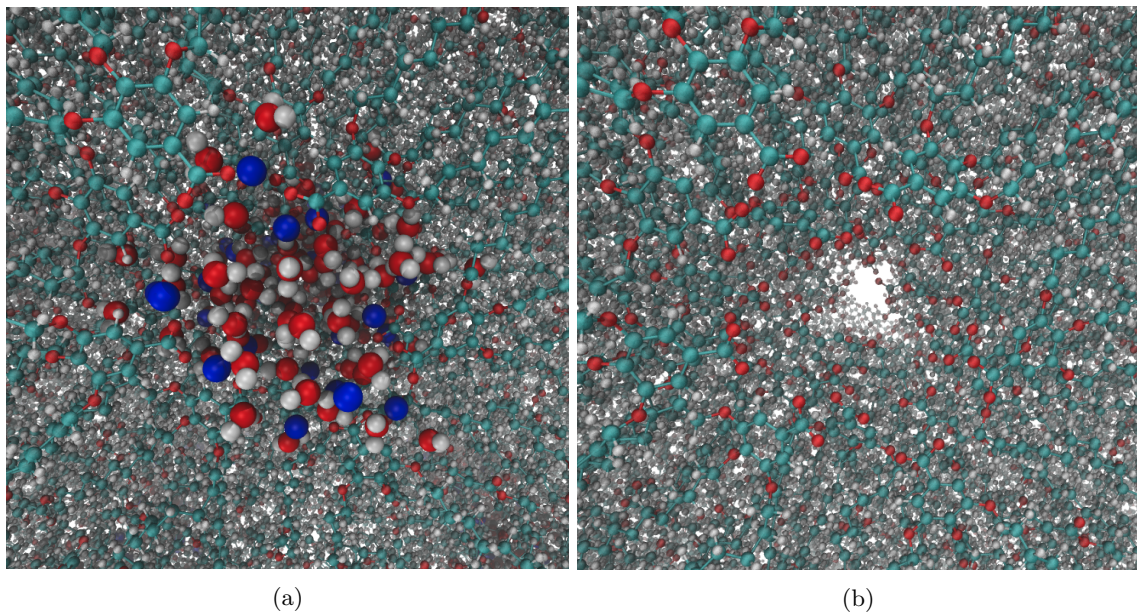


Figure 10: (a) Pores built in the parallel displaced configuration with 5 monomers per layer are filled with 5 wt% water. (b) The same system is visualized with water molecules and sodium ions removed. Head groups vacate the pore region leaving an aqueous solution of water and sodium ions.

## References

- [1] ChemAxon, “MarvinSketch 17.13 2017 ChemAxon (<http://chemaxon.com>),” 2017.
- [2] N. M. O’Boyle, M. Banck, C. A. James, C. Morley, T. Vandermeersch, and G. R. Hutchison, “Open Babel: An open chemical toolbox,” *Journal of Cheminformatics*, vol. 3, p. 33, Oct. 2011.
- [3] “The Open Babel Package, version 2.4.1 <http://openbabel.org>.”
- [4] J. Wang, W. Wang, P. A. Kollman, and D. A. Case, “Automatic atom type and bond type perception in molecular mechanical calculations,” *Journal of Molecular Graphics and Modelling*, vol. 25, pp. 247–260, Oct. 2006.
- [5] D. Case, R. Betz, W. Botello-Smith, D. Cerutti, T. Cheatham, III, T. Darden, R. Duke, T. Giese, H. Gohlke, A. Goetz, N. Homeyer, S. Izadi, P. Janowski, J. Kaus, A. Kovalenko, T. Lee, S. LeGrand, P. Li, C. Lin, T. Luchko, R. Luo, B. Madej, D. Mermelstein, K. Merz, G. Monard, H. Nguyen, H. Nguyen, I. Omelyan, A. Onufriev, D. Roe, A. Roitberg, C. Sagui, C. Simmerling, J. Swails, R. Walker, J. Wang, R. Wolf, X. Wu, L. Xiao, D. York, and P. Kollman, “AmberTools16,” Apr. 2016.
- [6] R. Walker and S. Tang, “Antechamber Tutorial ([ambermd.org/tutorials/basic/tutorial4b/](http://ambermd.org/tutorials/basic/tutorial4b/))”
- [7] A. W. Sousa da Silva and W. F. Vranken, “ACPYPE - AnteChamber PYthon Parser interfacE,” *BMC Research Notes*, vol. 5, p. 367, July 2012.